

# Food & Function

Accepted Manuscript



This is an *Accepted Manuscript*, which has been through the Royal Society of Chemistry peer review process and has been accepted for publication.

*Accepted Manuscripts* are published online shortly after acceptance, before technical editing, formatting and proof reading. Using this free service, authors can make their results available to the community, in citable form, before we publish the edited article. We will replace this *Accepted Manuscript* with the edited and formatted *Advance Article* as soon as it is available.

You can find more information about *Accepted Manuscripts* in the [Information for Authors](#).

Please note that technical editing may introduce minor changes to the text and/or graphics, which may alter content. The journal's standard [Terms & Conditions](#) and the [Ethical guidelines](#) still apply. In no event shall the Royal Society of Chemistry be held responsible for any errors or omissions in this *Accepted Manuscript* or any consequences arising from the use of any information it contains.

1 **Physicochemical properties and adsorption of cholesterol by**  
2 **okra (*Abelmoschus esculentus*) powder**

3

4

5

Yi Chen, Bing-Cheng Zhang, Yu-Han Sun, Jian-Guo Zhang, Han-Ju Sun and

6

Zhao-Jun Wei\*

7

8

School of Biotechnology and Food Engineering, Hefei University of Technology,

9

Hefei230009, People's Republic of China

10

11

12

\* Correspondence: Z.-J. Wei, School of Biotechnology and Food Engineering, Hefei

13

University of Technology, Hefei 230009; People's Republic of China. Tel:

14

86-551-62901539. Fax: 86-551-62901539. E-mail: [zjwei@hfut.edu.cn](mailto:zjwei@hfut.edu.cn)

15 **Abstract:** Okra (*Abelmoschus esculentus*) is widely used medicine purpose and as  
16 functional food. In order to clarify the effects of particle size on its functional  
17 properties, okra pods were subjected to superfine grinding and its properties were  
18 determined using different methods. Four particle size levels of okra powders were  
19 prepared- 380 to 250, 250 to 75, 75 to 40 and less than 40 $\mu$ m. The results showed that  
20 superfine grinding technology could efficiently pulverize the particles into submicron  
21 scale, whose distribution was close to a Gaussian distribution. With okra powder size  
22 diminishing, specific surface area, the water holding capacity (WHC), water-retention  
23 capacity (WRC), oil-binding capacity (OBC), tapped density and total flavonoids  
24 extraction were increased significantly ( $p<0.05$ ). Moreover, the adsorption of  
25 cholesterol by okra powder was improved after superfine grinding. These results  
26 suggest that okra powder could be used in the food manufacturing as a functional  
27 food ingredient..

28 **Keywords:** *Abelmoschus esculentus*, superfine grinding powder, physicochemical  
29 properties, adsorption of cholesterol

## 30 **Introduction**

31 *Abelmoschus esculentus*, indigenous to Africa, is usually known as okra and  
32 cultivated in many parts of the world including Middle East, the southern part of the  
33 USA and China<sup>1</sup>. Due to the rich amount of vitamins, dietary fiber and minerals, okra  
34 pods have been used as functional food ingredient as well as in traditional Chinese  
35 medicine for promoting diuresis and treatment of dental diseases and gastric  
36 irritations<sup>2</sup>. The health promoting properties of okra are suggested to reside in its  
37 non-starchy polysaccharides that are highly viscous and slimy when extracted with  
38 water.<sup>3,4</sup> Chemical composition analyses of okra have reported it to be rich in K, Na,  
39 Mg, and Ca with traces of Fe, Zn, Mn, and Ni.<sup>5</sup> In some countries okra fruits are also  
40 dried and stored for later use.

41 Micronization is a process of reducing the average diameter of a solid material's  
42 particles.<sup>6</sup> The size has a profound effect on the physicochemical characteristics of  
43 powder. It is usually effective to grind the biomaterials into superfine powders (i.e.  
44 ultrafine powder) for efficient extraction.<sup>7</sup> Numerous similar unit-operations have  
45 been developed in biological powder technology over the past decades due to the  
46 rapid and steady development of superfine powder techniques.<sup>8</sup> Compared with the  
47 samples ground with traditional methods, ultrafine particles bear the outstanding  
48 physical properties like dispersibility and solubility.<sup>9</sup> With the particle size decreasing,  
49 the surface of ultrafine powder can undergo some changes, which have brought out  
50 extraordinary characteristics that crude particles do not possess, including surface  
51 effect, mini-size effect, macro quantum channel effect, quantum effect, optical

52 property, mechanical property, magnetic property, chemical and catalytic property.  
53 Because of these notable characteristics, ultrafine powders have found many  
54 applications in ceramics, electric materials, chemicals and papermaking fields.<sup>10, 11</sup>

55 Applying micronization or nanotechnology in food and pharmaceutical industries  
56 has gained much attention. The fiber size of superfine grinding rice straw powder  
57 promotes enzymatic hydrolysis due to the cellulose accessibility.<sup>12</sup> The superfine  
58 ginger powder exhibits the good fluidity, water holding capacity, water solubility  
59 index and protein solubility.<sup>13</sup> The superfine powder of mushroom (*Agrocybe*  
60 *chaxingu* Huang) also exhibits good fluidity, water holding capacity and solubility,  
61 and is well suited to manufacture instant and convenient foods.<sup>14</sup> The ultrafine  
62 grinding has been suggested as a good way to fractionate biomaterials into easily  
63 bio-converted and hydrolyzed part.<sup>15</sup>

64 To date, the information available on the effect of the particle size on  
65 physical-chemical properties of okra are limited. The present research was, therefore,  
66 designed to investigate the application of the superfine grinding technology on okra  
67 pods and the effects of particle size on its functional properties.

## 68 **Materials and methods**

### 69 **Materials**

70 Okra pods were obtained from the Hanhua company in LuAn city, Anhui  
71 Province, China. Pods were sorted, cleaned, seeds removed and cut into small pieces.  
72 The pieces were dried in an electric thermostatic drying oven at 40 °C till the water  
73 content was less than 10% (w/w). The water content was determined by using AACC

74 method No. 44–19.<sup>16</sup>

### 75 **Preparation of okra powders**

76 A flow diagram of the okra powder procedure is shown in Fig.1. The dried okra  
77 pods were first milled to coarse particles by a disc-mill, and then screened through  
78 different sized sieves (40 and 60 Mesh, GB/T6003.1-1997) to separate granules ( $d <$   
79  $380\mu\text{m}$ ). The superfine powders were obtained by using high pressure pulverizer  
80 (Huanyatianyuan Machinery Company, Beijing, China), which were subdivided  
81 through different sized sieves (200 and 350 mesh, GB/T6003.1-1997)

### 82 **Particle size and color difference analysis**

83 Particle size distributions were determined by laser granulometry with a Malvern  
84 Mastersizer 2000 diffraction laser particle sizer (Malvern, Malvern Instruments Ltd,  
85 UK). All determinations were performed in triplicate. The instrument provides  
86 volume weighted size distributions and particle size parameters, such as volume  
87 median diameter ( $d_{50}$ ), De Brouckere mean diameter ( $d_{43} = \frac{\sum n_i d_i^4}{\sum n_i d_i^3}$ ), and  
88 Sauter mean diameter ( $d_{32} = \frac{\sum n_i d_i^3}{\sum n_i d_i^2}$ ), where  $n_i$  is the number of droplets of  
89 diameter  $d_i$ .

90 Median diameter is the value of the particle size which divides the population  
91 exactly into two equal halves i.e. there is 50% of the distribution above this value and  
92 50% below. Median diameter is especially important in case of a bimodal distribution.  
93 De Brouckere mean diameter is the volume or mass mean diameter of the particles,  
94 and Sauter mean diameter is the surface area weighted mean diameter of the particles.

95 17

96 Color difference, as indicators being 'L', 'a' and 'b' of the okra powders, was  
97 determined on a WB-2000IX A-automatic color difference meter (Shanghai Exact  
98 Science Instrument Ltd., Shanghai, China).

### 99 **Scanning electron microscope (SEM)**

100 Morphological characterization of okra powders was performed using images  
101 acquired by SEM Quanta 200FEG-SEM (FEI Co. Netherlands) at 150 kV accelerated  
102 voltage and 10–15 mm working distance. The samples were coated with platinum of  
103 10 nm thicknesses to make the samples conductive.

### 104 **Bulk density, tapped density and repose angle**

105 The bulk density (g/mL) refers to density including pores and interparticle voids.  
106 The bulk density of okra powder was calculated as follows:<sup>18</sup>

$$107 \quad \mathbf{B} = \frac{W_2 - W_1}{10} \quad (1)$$

108 Where  $W_2$  was the total weight of okra pods powder and 10 mL measuring cylinder,  
109 and  $W_1$  was the weight of the 10mL measuring cylinder. All measurements were  
110 performed in triplicate.

111 The tapped density was determined according to the method of Usp32-616<sup>19</sup>.

112 Calculate the tapped density by the formula:

$$113 \quad \mathbf{T} = \frac{M}{V_0 - V_1} \quad (2)$$

114 Where  $M$  was the total weight of okra pods powder, and  $V_0$  was the unsettled

115 apparent volume,  $V_1$  was the tapped volume. All measurements were performed in  
116 triplicate.

117 Repose angle was determined according to the method of Zhang et al.<sup>14</sup>. A filler  
118 was fixed above a glass plane so that the height (H) of the glass plane from the outlet  
119 of the filler was 1 cm, and the filler was vertical to the glass plane. The okra powders  
120 were poured into the filler separately until the tip of the powder cones that they  
121 formed on the plane exactly touched the outlet of the filler. The radius (R) of the cone  
122 was measured for each type of powder. Repose angle ( $\alpha$ ) was calculated using Eq.  
123 (3)<sup>20</sup>.

$$124 \quad \alpha = \tan^{-1} \frac{H}{R} \quad (3)$$

### 125 **Swelling capacity**

126 Swelling property is defined as the ratio of the volume occupied when the sample  
127 is immersed in excess of water after equilibration to the actual weight. Accurately  
128 weighed dry sample (0.2 g) was placed in a graduated test tube, around 10mL of water  
129 was added and it was hydrated for 18 h. After 18 h, the final volume attained by  
130 powder was measured.<sup>21</sup>

$$131 \quad \text{Swelling capacity (mL/g)} = \frac{\text{volume occupied by sample}}{\text{original sample weight}} \quad (4)$$

### 132 **Water holding capacity and water-retention capacity**

133 The water holding capacity was determined, using the method of Anderson<sup>22</sup>. First,  
134 the weights of empty centrifuge tubes (M) and different sized okra powders ( $M_1$ ) were

135 measured. Then the powders ( $M_1$ ) were dispersed in water at a ratio of 0.05:1 at 20°C  
136 in centrifuge tube(M), which were placed in a water bath at 60°C. The tubes were  
137 incubated for 60 min, after that moved to cold water for 30 min, followed by  
138 centrifugation for 20 min at 5000 rpm. The supernatant was removed and the  
139 centrifuge tubes with the powders ( $M_3$ ) were weighed. The formula to calculate water  
140 holding capacity (WHC) is as follows:

$$141 \quad \text{WHC}(\text{g/g}) = \frac{M_3 - M - M_1}{M_1} \quad (5)$$

142 The water-retention capacity (WRC) was defined as the quantity of water that  
143 remains bound to the hydrated fiber following the application of an external force  
144 (pressure or centrifugation). The WRC was determined according to the description  
145 by Raghavendra et al. (2004)<sup>21</sup> with modifications. The different size powders ( $W_1$ )  
146 were dispersed in water with a ratio of 0.05:1 at 20°C, placed in centrifuge tubes  
147 which were incubated in a shaker water bath (100rpm) maintained at 80°C, then  
148 shook it for 60 min at 100r/min. At the end of incubation, mixture was centrifuged at  
149 6000 rpm for 10 min, the supernatant was removed and the residue weight was  
150 recorded ( $W_2$ ). The samples were then weighed ( $W_3$ ) again when being dried at  
151 105°C.

$$152 \quad \text{WRC}(\text{g/g}) = \frac{W_2 - W_3}{W_1} \quad (6)$$

### 153 Oil-binding capacity (OBC)

154 OBC is determined by the method of Sangnark and Noomhorm<sup>23</sup> with slight  
155 modifications. The dried okra powders (1.0 g) were mixed with soybean oil (20 mL)

156 in centrifuge tubes and left for 1h at 37 °C, respectively. The mixtures were then  
157 centrifuged at 1,500g for 10min, the supernatants decanted and the pellet was  
158 recovered by filtration through a nylon mesh. OBC was expressed as follows: <sup>24</sup>

$$159 \quad \text{OBC(g/g)} = \frac{\text{Pellet weight-Original dryweight}}{\text{Original dryweight}} \quad (7)$$

### 160 **Flavonoids Extraction**

161 The extraction and determination of flavonoids were carried out, by the method of  
162 Cui et al (2013)<sup>25</sup> with some modifications. Okra powders (3 g) were placed into an  
163 Erlenmeyer flask (100 mL) with 30mL diethyl ether solvent for 12h to remove  
164 lipophilic impurities. Then, the ether was removed by suction filtration. Ethanol was  
165 added (95%, v/v; liquid to solid ratio 50:1, mL/g) into the Erlenmeyer flask that was  
166 sonicated in an ultrasonic cleaning bath for 2h at 60 °C. After the extract was filtered,  
167 the evaporated filtrate was used for the determination of the flavonoids. The diluted  
168 sample (1 mL) containing flavonoids was mixed with 0.3 mL of 5% (w/v) sodium  
169 nitrite, 0.3 mL of 10% (w/v) aluminum nitrate and 4 mL of 4% (w/v) sodium  
170 hydroxide, and the final volume was adjusted to 10 mL with 70% (v/v) ethanol. After  
171 allowing the mixture to stand 15min at room temperature, the absorbance of the  
172 solution at 510 nm was determined with a UV752 spectrophotometer. Flavonoid  
173 concentration was calculated using rutin as standard. The calibration curve ( $y =$   
174  $-0.0004+18.538x$ , where  $y$  is absorbance value at 510 nm of sample,  $x$  is flavonoids  
175 concentration) ranged 0.0104–0.0520mg/mL ( $R^2 = 0.9999$ ).

### 176 **Adsorption capacity of okra powder for cholesterol**

177 Adsorption of cholesterol by okra powder was estimated from the change in  
178 cholesterol concentration on exposure of the solution to the powders. Increasing  
179 concentrations of cholesterol solutions were made in glacial acetic acid. A known  
180 concentration of cholesterol solution was max with and known amount of okra  
181 powder and the mixture was in a shaker water bath (90 rpm) maintained at 37 °C for  
182 60min. A flask without any okra powder served as blank control. At the end of  
183 adsorption, a 2 mL volume of the supernatant was taken for cholesterol estimation.

184 The determination on content of cholesterol in solution was detected according to  
185 the national standards (GB/T 15206-94). The calibration curve ( $y = 15.469x + 0.0065$ ,  
186 where  $y$  is absorbance value at 563nm of sample,  $x$  is cholesterol concentration)  
187 ranged 0.0125–0.0625mg/mL ( $R^2 = 0.9996$ ).

188 The formula to calculate adsorption capacity (CAC) for cholesterol is as follows:

$$189 \quad CAC(\text{mg/g}) = \frac{V(\rho_0 - \rho - \rho_k)}{m} \quad (8)$$

190 Where  $m$  was the total weight of okra pods powder;

191  $V$  was the volume of the cholesterol solution;

192  $\rho_0$  and  $\rho$  were the concentrations of the cholesterol solution before and after  
193 absorbing, respectively;

194  $\rho_k$  was the concentration of the cholesterol solution in the blank control.

195 All measurements were performed in triplicate.

196 In vitro sorbent testing was carried out in series of single factor tests to study how  
197 factors, such as the particle size of powder, temperature, absorption time and the  
198 initial concentration of cholesterol influence the sorption process. In order to

199 characterize the adsorption process, the experimental data were fitted with adsorption  
200 isotherms and analyzed by thematics.

### 201 **Statistical analysis**

202 All determinations were carried out in triplicates. The data are presented as mean+/-  
203 SD and analyzed statistically using Analysis of variance. Statistical significance was  
204 considered at  $p < 0.05$ .

## 205 **Results and discussion**

### 206 **Surface properties**

207 The different size okra powders had different surface properties (Table 1). Different  
208  $d_{43}$  values of coarse powder and superfine samples were 359.021, 273.31, 69.373 and  
209 23.110  $\mu\text{m}$ , respectively (Table 1). Okra powder with the smallest granule size (18.69  
210  $\mu\text{m}$ ) was found to have the highest specific surface area as 0.824  $\text{m}^2/\text{g}$ , lowest  $d_{43}$  and  
211  $d_{32}$ , respectively. Inversely, the okra powder with the largest particles (349.6  $\mu\text{m}$ ) had  
212 the lowest specific surface (0.096  $\text{m}^2/\text{g}$ ), highest  $d_{43}$  and  $d_{32}$ , respectively (Table 1).

213 Therefore, superfine grinding technology could efficiently pulverize the particles to  
214 submicron scale. Furthermore, the particle size distribution was close to a Gaussian  
215 distribution. Finer particles tended to have a greater number of particles per unit  
216 weight. It was an indication of a higher potential for achieving homogeneity when  
217 mixing with the active pharmaceutical ingredient and other powder additives.<sup>26</sup> The  
218 higher specific surface area of the finer particles also can improve the adsorption  
219 capacity, which would be discussed in the following content. The specific surface area

220 and moisture adsorption tendency may have an indirect effect on drug dissolution  
221 from solid dosage forms.<sup>26</sup>

### 222 **Colour differences**

223 The color is an important quality of all foods including, food powders. The previous  
224 investigation indicated that the particle size had a significant effect on lightness of red  
225 pepper powder.<sup>27</sup> The colors were expressed as L indicates lightness, while a and b are  
226 chromaticity coordinates; +a is in the red direction, -a is in the green direction, +b is  
227 in the yellow direction, and -b is in the blue direction<sup>28</sup>. The data presented in Table 2  
228 show that the particle size affects the color of okra powder slightly. We observed that  
229 'a' increased steadily with decreasing particle size of okra powder. And 'L' increased  
230 from the grade 380-250 $\mu\text{m}$  to 250-75 $\mu\text{m}$ , while 'b' increased dramatically from the  
231 grade 250-75 $\mu\text{m}$  to 75-40 $\mu\text{m}$ . As the specific surface area increased, the particles  
232 become more homogeneous, with increased exposure of inside material, which  
233 affected the color of the powder.

### 234 **Bulk density, tapped density and repose angle**

235 Because the inter-particulate interactions influence the bulking properties of powder  
236 and also interferes with powder flow, a comparison of the bulk and tapped densities  
237 can give a measure of the relative importance of these interactions in a given powder.  
238 Such a comparisons are often used as an index of the ability of the powder to flow.<sup>19</sup>  
239 As particle size of okra powder decreased, bulk density reduced from 0.4718 to  
240 0.2941 g/mL (Table 3). The bulk density of okra powder (0.4718 g/mL) with the

241 particle size of 380-250  $\mu\text{m}$  was the largest. Whereas, the tapped density of okra  
242 powders increased from 0.6813 to 3.3787 g/mL with the decrease of particle size  
243 (Table 3). The okra particle of the higher tapped density was beneficial to fill in  
244 preparing tablets or capsule products.<sup>29</sup>

245 The powders showed different fluidity when tested for angle of repose as shown in  
246 Table 3. From the Table 3, it is obvious that the smaller the powder particle was, the  
247 smaller was the angle of repose. The angle of repose ranged from 56.35° (380-250  $\mu\text{m}$ )  
248 to 46.58° (<40  $\mu\text{m}$ ) (Table 3). These results confirmed the significant effect of the  
249 particle size on the angle of repose. The okra powder with least particle size had the  
250 lowest angle of repose (46.58°). On the contrary, okra powder with a particle size of  
251 380-250  $\mu\text{m}$  had the largest angle of repose (56.35°). With decreasing angle of repose,  
252 one should expect a better fluidity of granular bulk.<sup>30</sup>

### 253 **Microphotographs of okra powder**

254 The morphology of fragmented okra pods granules could be seen clearly in the  
255 scanning electron microscope photos (Fig.2). Mechanical damage exhibited  
256 transformation from an ordered structure to a disordered structure via the breakage of  
257 intermolecular bonds.<sup>31</sup> We observed granular mechanical damage in broken okra  
258 pods granules. Extensive milling broke the coarse particles into finer fractions, with  
259 the combination of flattening, aggregation and rupture resulted in various shapes of  
260 okra pods particles, as could be seen in Fig. 2. The shape of the superfine pulverous  
261 particle (40 and 75  $\mu\text{m}$ ) by the mill was not round. It was lamellar peeling in shape.  
262 The okra fiber was totally broken by the strong mechanical pressure and abrasion

263 between rubbing rings and inner bottom of pot.

#### 264 **The hydration properties and OBC**

265 As shown in Table.4, the WHC, WRC, SC and OBC increased as the size of okra  
266 particles decreased. The WHC values of okra powder with particle sizes of 380–40  
267  $\mu\text{m}$  ranged from 3.55 to 8.24g/g respectively (Table.4). The hydration properties  
268 increased with the decrease of particle size. This may be because properties of the fine  
269 were altered, e.g., increased surface area and surface energy, with grinding. Moreover,  
270 grinding the dry fibrous material to fine powder may leads to large changes in the  
271 fiber matrix structure.<sup>32</sup> Similarly, the SC of powder was 1.22, 1.53, 1.24, and 1.27 g/g,  
272 respectively. The higher SC of okra powders suggests their potential use as an  
273 ingredient of instant foods.

#### 274 **The effects on total flavonoid extract**

275 The superfine milling could cause significant differences in chemical composition  
276 separation of the granulometric fractions.<sup>33</sup> The data on solubility of flavonoids of  
277 okra in different size particles are presented in Fig.3. These data show that the  
278 solubility of flavonoids increased as the particle size decreased. This suggested that  
279 the smaller the size, higher the content of flavonoids. The flavonoids solubility of okra  
280 pods powder with particle sizes of 380–40  $\mu\text{m}$  were from 3.269% to 7.251%. The  
281 main factor to affect the solubility of flavonoids was shown to be the particle size and  
282 the surface area of the powder.

#### 283 **Effects on cholesterol adsorption capacity of okra powder**

284 Fig.4 showed the effect of four factors (particle size, temperature, initial concentration  
285 and absorption time) on cholesterol absorption capacity of okra powder. As can be  
286 seen in Fig. 4A, the adsorption capacity increased with the decrease in grain-size. The  
287 higher specific surface area of the fine particles leads to the larger contact area, which  
288 shortened the path distance for absorbing. It is well-known that the temperature  
289 usually has great influence on the adsorption because it affects the dispersion of the  
290 powder, concentration of the cholesterol which lies on the functional groups of the  
291 adsorbents in the adsorption process. Lower temperature was conducive to adsorption  
292 powder (Fig. 4B). The initial concentration of cholesterol has been proved as a key  
293 factor which can be illustrated in Fig. 4C, exhibiting a dose-dependence tendency. The  
294 experimental results in Fig. 4D displayed that the adsorption increased with the  
295 contact time from 10 to 60 min reaching a plateau over the next of 60–90 min. It  
296 should be pointed out that the adsorption of cholesterol is a fast process that can  
297 remove more than 80% cholesterol from aqueous solution in the short time interval of  
298 less than 15 min.

### 299 **Adsorption isotherms and thermotics analysis**

300 To examine the relationship between the sorption capacity ( $q_e$ ) and the concentration  
301 of cholesterol at equilibrium ( $C_e$ ), experimental data are fitted to Langmuir,  
302 Freundlich and Dubinin-Radushkevish (D-R) isotherms models. These three models  
303 are widely used for adsorption data analysis, since they have the ability to describe  
304 experimental results for a wide range of initial concentrations. Langmuir<sup>34</sup> and  
305 Freundlich<sup>35</sup> adsorption isotherms are also classical models for describing equilibrium

306 between adsorbate adsorbed onto the sorbent and adsorbate remaining in solution at  
307 equilibrium at a constant temperature.

308 The theoretical Langmuir isotherm relies on the chemical or physical interaction (or  
309 both) postulated to occur between the solute and the available vacant sites on the  
310 sorbent surface, which may be described as below:

$$311 \quad \frac{1}{q_e} = \frac{1}{Q_m K_L} \times \frac{1}{C_e} + \frac{1}{Q_m} \quad (9)$$

312 where  $Q_m$  is the maximum concentration of the sorbent (mg/g),  $C_e$  is the equilibrium  
313 concentration (mg/mL), and  $K_L$  is a coefficient related to the affinity between the  
314 adsorbate and the sorbent.

315 The Freundlich isotherm is an empirical equation that is based on the sorption of a  
316 sorbate on a heterogeneous surface of a sorbent as given by the equation:<sup>36</sup>

$$317 \quad \ln q_e = \ln K_f + \frac{1}{n} C_e \quad (10)$$

318 where  $K_f$  and  $n$  are the Freundlich empirical constants indicative of sorption capacity  
319 and sorption intensity, respectively.

320 The Dubinin-Radushkevich (D-R) model, which does not assume a homogeneous  
321 surface or a constant biosorption potential as the Langmuir model, was also used to  
322 test the experimental data. The D-R isotherm can be written as:<sup>37</sup>

$$323 \quad \ln q_e = \ln q_m - k\xi^2 \quad (11)$$

324 where  $k$  is a coefficient related to the mean free energy of adsorption ( $\text{mol}^2/\text{kJ}^2$ ),  $q_m$  is  
325 the maximum adsorption capacity and  $\xi$  is the Polanyi potential ( $\text{kJ/mol}$ ) that can be  
326 written as :

$$327 \quad \xi = RT \ln\left(1 + \frac{1}{C_0}\right) \quad (12)$$

328 The mean free energy of biosorption,  $E$ , can be estimated using the following  
329 equation:

$$330 \quad E = -\frac{1}{\sqrt{2k}} \quad (13)$$

331 Experimental data from curves given in Table 5 were used Eq. (9),(10) and (11),  
332 allowing us to determine kinetic parameters. According to the regression coefficient  
333 values  $R^2$  in Table 5, it can be pointed out that the adsorption isotherms can be fairly  
334 described by the Langmuir equation rather than the Freundlich one. And the parameter  
335  $|E|$  from the D-R isotherm model is  $3.595 < 8 \text{ kJ/mol}$ , which demonstrate the energy of  
336 activation. It illustrate the physical adsorption might be a dominant mechanism  
337 involved in adsorption by okra powder.<sup>38,39</sup>

338 The character of Langmuir isotherm can also be described by the balance coefficient  
339  $R_L$ ,<sup>40</sup> which may be described as below:

$$340 \quad R_L = \frac{1}{1 + K_e C_0} \quad (14)$$

341 where  $K_e$  and  $C_0$  are the Langmuir empirical constants indicative of sorption capacity  
342 and the initial concentration of cholesterol, respectively.

343 Fig.5 present the change of balance coefficient  $R_L$  with the initial concentration of  
344 cholesterol. As can be seen, the value of  $R_L$  is between 0 and 1, which shows the  
345 adsorption property of okra powder is considered to be favorable.<sup>41</sup> In other words,  
346 okra superfine powder is a suitable biosorbent .

347 The thermotics properties of adsorption is analyzed with Gibbs free energy  $\Delta G$ ,

348 adsorption enthalpy variation  $\Delta H$ , adsorption entropy variation  $\Delta S$ .

349 The adsorption balance coefficient  $K_e$ , which be described as below:

$$350 \quad K_e = \frac{C_e}{Q_e} \quad (15)$$

351 The  $\Delta G$  can be estimated using the equation according to the classical Van't Hoff  
352 equation:

$$353 \quad \Delta G = -RT \ln K_e \quad (16)$$

354 The mutual relation among  $\Delta G$ ,  $\Delta H$  and  $\Delta S$  is showed as bellow: <sup>42</sup>

$$355 \quad \Delta H = \Delta G + \Delta S \times T \quad (17)$$

356 Where R and T are ideal gas constant ( $8.314 \times 10^{-3} \text{kJ}/(\text{mol} \cdot \text{K})$ ) and adsorption  
357 temperature (K).

358 Eq. (16) and (17) can derive to the following:

$$359 \quad \ln K_e = \frac{\Delta S}{R} - \frac{\Delta H}{RT} \quad (18)$$

360 Fit the experiment data to the equation (18), and the values of  $\Delta G$ ,  $\Delta H$  and  $\Delta S$   
361 obtained are showed in Table. 6. Based on the results, the Gibbs free energy  $\Delta G$   
362 increases with the temperature rise, which indicate that the lower temperature is  
363 conducive to the sorption process. Besides, when the temperature is less than 323.15K,  
364 the  $\Delta G$  is less than zero, which means the adsorption is spontaneous.<sup>43</sup> The adsorption  
365 is exothermic, which could be confirmed by the adsorption enthalpy variation  $\Delta H$   
366 being less than zero.

367 **Conclusion**

368 In this study, the physicochemical properties and adsorption of cholesterol by four  
369 sizes of okra powder obtained by micronization were investigated. The results showed  
370 the particle size significantly influenced the properties of okra powder. With the size  
371 decreasing, the specific surface area, bulk density, tapped density, repose angle,  
372 hydration properties, oil-binding capacity performed better and the extraction of  
373 flavonoid increased notably. What's more, the powder showed a better binding  
374 capacity for cholesterol with the particle size diminishing. The adsorption equilibrium  
375 data followed the Langmuir adsorption isotherm. The results indicated the promising  
376 potential of the superfine okra powder to be a cholesterol sorbent or an alternative  
377 source with additional benefits in function food. The effects of particle size on the  
378 physical-chemical properties provide a theoretical base and reference for potential  
379 using of okra in the food industry.

### 380 **Acknowledgments**

381 This study is supported by the National Natural Science Foundation of China  
382 (31171787), and the National Training Programs of Innovation and Entrepreneurship  
383 for Undergraduates (201410359055).

384 **References**

- 385 1. N. Sengkhampan, R. Verhoef, H. A. Schols, T. Sajjaanantakul and A. G.  
386 Voragen, *Carbohydr. Res.*, 2009, **344**, 1824-1832.
- 387 2. R. Ndjouenkeu, F. Goycoolea, E. Morrissa and J. Akingbala, *Carbohydr. Polym.*,  
388 1996, **29**, 263-269.
- 389 3. Y. Chen, J.G. Zhang, H.J. Sun and Z.J. Wei, *Int. J. Biol. Macromol.*, 2014, **70**,  
390 498-505.
- 391 4. P. Gunness and M. J. Gidley, *Food Func.*, 2010, **1**, 149-155.
- 392 5. Y. Zhou, X. Jia, J. Shi, Y. Xu, L. Jing and L. Jia, *Helv. Chim. Acta*, 2013, **96**,  
393 533-537.
- 394 6. F. Zhu, B. Du, R. Li and J. Li, *Biocatal. Agric. Biotechnol.*, 2013.
- 395 7. T.Q. Chen, Y.B. Wu, J.G. Wu, L. Ma, Z.H. Dong and J.Z. Wu, *J. Taiwan Inst.*  
396 *Chem. Eng.*, 2013.
- 397 8. X.Y. Zhao, Q. Ao, L.W. Yang, Y.F. Yang, J.C. Sun and G.S. Gai, *J. Taiwan Inst.*  
398 *Chem. Eng.*, 2009, **40**, 337-343.
- 399 9. K. Tkacova and N. Stevulova, *Freiberger Forsch. A (Partik.) A*, 1998, **841**,  
400 14-25.
- 401 10. W. Miao, *US Patent 20,030,234,304*, 2003.
- 402 11. L.L. Song, B.Y. Fan, S.Z. Jiang and D.L. Zhang, *Zhongguo Zhong Yao Za Zhi*,  
403 2002, **27**, 12-15..
- 404 12. S. Jin and H. Chen, *Biochem. Eng. J.*, 2006, **30**, 225-230.
- 405 13. X. Zhao, Z. Yang, G. Gai and Y. Yang, *J. Food Eng.*, 2009, **91**, 217-222.

- 406 14. M. Zhang, C.J. Zhang and S. Shrestha, *J.Food Eng.*, 2005, **67**, 333-337.
- 407 15. L.H. Zhang, H.D. Xu and S.F. Li, *Innov. Food Sci. Emerg.*, 2009, **10**, 633-637.
- 408 16. HosneyRC. Breakfast cereals. In AACC International, editor. Principles of  
409 cereal science and technology. St Paul, MN, American Association of Cereal  
410 Chemists, 2000.
- 411 17. S. Protonotariou, A. Drakos, V. Evageliou, C. Ritzoulis and I. Mandala, *J.*  
412 *Food Eng.*, 2014,24-29.
- 413 18. Y. X. Bai and Y.F. Li, *Carbohydr. Polym.*, 2006, **64**, 402-407.
- 414 19. U. Pharmacopeia, *Rockville: USP*, 2006, 2638.
- 415 20. H. Wang, Y. Chen and P. Ma, *Chin. New Drugs J.*, 2006, **15**, 1535.
- 416 21. S. N. Raghavendra, N. K. Rastogi, K. S. M. S. Raghavarao and R. N.  
417 Tharanathan, *Eur. Food Res. Technol.*, 2004, **218**, 563-567(565).
- 418 22. R. Anderson, *Cereal Chem.*, 1982, **59**.
- 419 23. A. Sangnark and A. Noomhorm, *Food Chem.*, 2003, **80**, 221-229(229).
- 420 24. J. Nsor-Atindana,F. Zhong, K.J. Mothibe, *Food Funct.*, 2012, **3**, 1044-1050.
- 421 25. H.P. Cui, J.G. Zhang, Z. Dong and Z.J. Wei, *J. Food, Agric. Environ.*, 2013,  
422 **11(3&4)**, 413-419.
- 423 26. C. K. Riley, S. A. Adebayo, A. O. Wheatley and H. N. Asemota, *Powder*  
424 *Technol.*, 2008, **185**, 280-285.
- 425 27. Q. Chen, H. Koh and J. Park, *T. ASAE*, 1999, **42**, 749-752.
- 426 28. K. Liu, *Bioresource technol.*, 2008, **99**, 8421-8428.
- 427 29. F. Costa, A. Pais and J. Sousa, *Int. J. pharm.*, 2004, **270**, 9-19.

- 428 30. K. Ileleji and B. Zhou, *Powder Technol.*, 2008, **187**, 110-118.
- 429 31. X. Zhao, F. Du, Q. Zhu, D. Qiu, W. Yin and Q. Ao, *Powder Technol.*, 2010,  
430 **203**, 620-625.
- 431 32. K. Zhu, S. Huang, W. Peng, H. Qian and H. Zhou, *Food Res. Int.*, 2010, **43**,  
432 943-948.
- 433 33. C. Maaroufi, J.P. Melcion, F. De Monredon, B. Giboulot, D. Guibert and M.P.  
434 Le Guen, *Anim. Feed Sci. Technol.*, 2000, **85**, 61-78.
- 435 34. I. Langmuir, *Twelfth International Water Technology Conference*, 1918,  
436 1361-1403.
- 437 35. H. Freundlich, *Über die adsorption in lösungen*, 1906, **57A**, 385-470.
- 438 36. F. Banat and S. Al, *Adsorpt. Sci. Technol.*, 2003, **21**, 245-260.
- 439 37. M. Dubinin and L. Radushkevich, *Phys. Chem. Sect.*, 1947, **55**, 327.
- 440 38. F. G. Helfferich, *Ion exchange*, Courier Dover Publications, New York, 1962.
- 441 39. X. Tang, Z. Li and Y. Chen, *J. Hazard. Mater.*, 2009, **161**, 824-834.
- 442 40. T. W. Weber and R. K. Chakravorti, *AIChE J.*, 1974, **20**, 228-238(211).
- 443 41. X. Xu, B. Gao, W. Wang, Q. Yue, Y. Wang and S. Ni, *Colloids Surfaces. B.*,  
444 2009, **70**, 46-52.
- 445 42. T. S. Anirudhan and P. G. Radhakrishnan, *J. Chem. Thermodyn.*, 2008, **40**,  
446 702-709.
- 447 43. S. Hong, C. Wen, J. He, F. Gan and Y.-S. Ho, *J. Hazard. Mater.*, 2009, **167**,  
448 630-633.
- 449

450 **Figure captions**

451 **Fig.1** Flow diagram of the okra powder procedure

452 **Fig.2** SEM images of different particle size okra powders. (A) Particle size 380-250

453  $\mu\text{m}$ , 50 $\times$  ; (B) Particle size 250-75  $\mu\text{m}$ , 50 $\times$  ; (C) Particle size 75-40  $\mu\text{m}$ , 50 $\times$  ; (D)

454 Particle size <40  $\mu\text{m}$ , 500 $\times$  ; (E) Particle size 75-40  $\mu\text{m}$ , 1,000 $\times$  ; (F) Particle size

455 <40  $\mu\text{m}$ , 2,500 $\times$ .

456 **Fig.3** The change of the solubility percentage of flavonoids of different particle size

457 okra powders.

458 **Fig.4** The effect of particle size (A), temperature (B), initial concentration (C) and

459 absorption time (D) on cholesterol absorption capacity of okra powder

460 **Fig.5** The balance coefficient  $R_L$  for Langmuir isotherm

461

462 **Table 1** Physical characteristics of okra powder particles obtained from the laser  
463 diffraction method

Powder ( $\mu\text{m}$ )	Equivalent diameter particles accounted for by measuring the proportion ( $\mu\text{m}$ )					Specific surface area ( $\text{m}^2/\text{g}$ )
	$D_{10}$	$D_{50}$	$D_{90}$	$D(4,3)$	$D(3,2)$	
380-250	48.419	349.6	646	359.021	34.403	0.096
250-75	15.847	243.770	562.426	273.310	25.615	0.234
75-40	9.30	65.679	128.079	69.373	16.474	0.364
<40	3.61	18.690	49.273	23.110	7.285	0.824

464

465

466 **Table 2** Color difference of okra powders

Okra pods particle ( $\mu\text{m}$ )	L	a	b
380-250	60.21 $\pm$ 0.7891	6.58 $\pm$ 0.7670	14.93 $\pm$ 0.5749
250-75	64.9 $\pm$ 1.1223	7.58 $\pm$ 0.5908	18.05 $\pm$ 0.8741
75-40	65.21 $\pm$ 1.0729	8.25 $\pm$ 0.8757	24.98 $\pm$ 0.4588
<40	64.95 $\pm$ 0.8821	8.93 $\pm$ 1.7165	23.12 $\pm$ 0.2557

467

The data are mean $\pm$  standard deviation of triplicate samples.

468

469

470 **Table 3** Bulk density, tapped density and repose angle of different particle size okra  
471 pods powders

Okra pods particle ( $\mu\text{m}$ )	Bulk density (g/mL)	Tapped density (g/mL)	Repose angle ( $^{\circ}$ )
380-250	0.4718 $\pm$ 0.06	0.6813 $\pm$ 1.13	56.3582 $\pm$ 2.76
250-75	0.3562 $\pm$ 0.03	1.0374 $\pm$ 0.44	53.9147 $\pm$ 3.25
75-40	0.3042 $\pm$ 0.03	1.6669 $\pm$ 0.23	48.2771 $\pm$ 1.36
<40	0.2941 $\pm$ 0.01	3.3787 $\pm$ 0.01	46.5808 $\pm$ 1.30

472

473

474

**Table 4** Hydration properties and OBC of okra powders

Okra pods particle ( $\mu\text{m}$ )	WHC (g/g)	WRC (g/g)	Swelling capacity (mL/g)	OBC (g/g)
380-250	3.55 $\pm$ 0.7423	0.56 $\pm$ 0.0134	1.28 $\pm$ 0.0047	1.22 $\pm$ 0.0124
250-75	4.86 $\pm$ 0.5671	0.59 $\pm$ 0.0109	1.59 $\pm$ 0.0339	1.23 $\pm$ 0.1048
75-40	6.42 $\pm$ 0.0114	0.71 $\pm$ 0.0252	2.42 $\pm$ 0.0206	1.24 $\pm$ 0.0251
<40	8.24 $\pm$ 0.0907	0.77 $\pm$ 0.0271	2.79 $\pm$ 0.0072	1.27 $\pm$ 0.2126

475

476

477 **Table 5** Fitted isothermal adsorption models and their parameters

Isotherm model	Parameters	equation	R <sup>2</sup>	
Langmuir isotherm	Q <sub>m</sub>	0.891±0.0570	$1/q_e = 0.318/C_e + 1.122$	0.95
	K <sub>e</sub>	3.528±0.479		
Freundlich isotherm	1/n	0.460±0.1039	$\ln Q_e = 0.46C_e - 0.854$	0.805
	K <sub>f</sub>	0.426±0.1088		
D-R isotherm	q <sub>m</sub>	1.295±0.06311	$\ln q_e = -0.0387\xi^2 - 0.2588$	0.969
	K	0.0387±0.0235		
	E	-3.595		

478

479

480 **Table 6** Thermodynamic parameters for cholesterol adsorption

Temperature/K	$\Delta G$ /(kJ/mol)	$\Delta H$ /(kJ/mol)	$\Delta S$ /(J/(mol·K))
293.15	-6.236		
303.15	-2.984		
313.15	-0.614	-62.765	-195.454
323.15	0.328		
333.15	1.713		

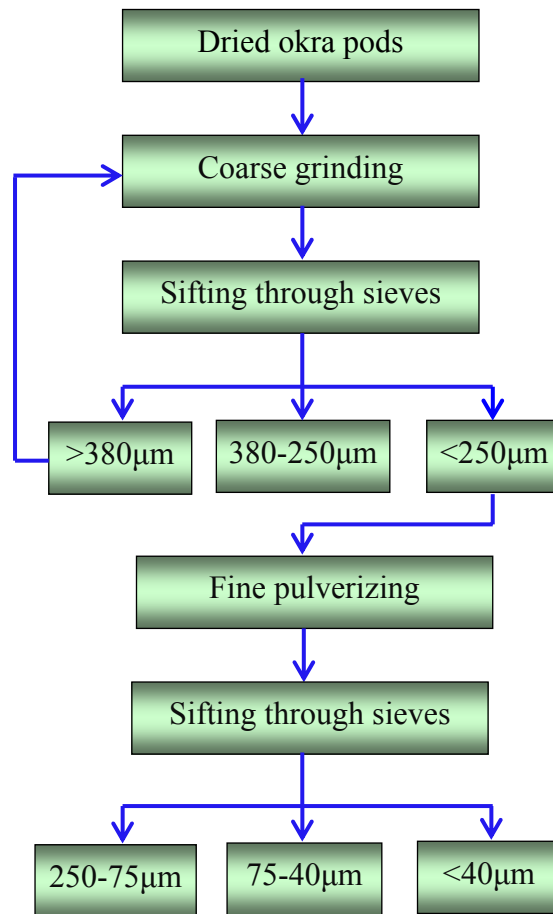
481

482

483 **Fig.1** Flow diagram of the okra powder procedure

484

485

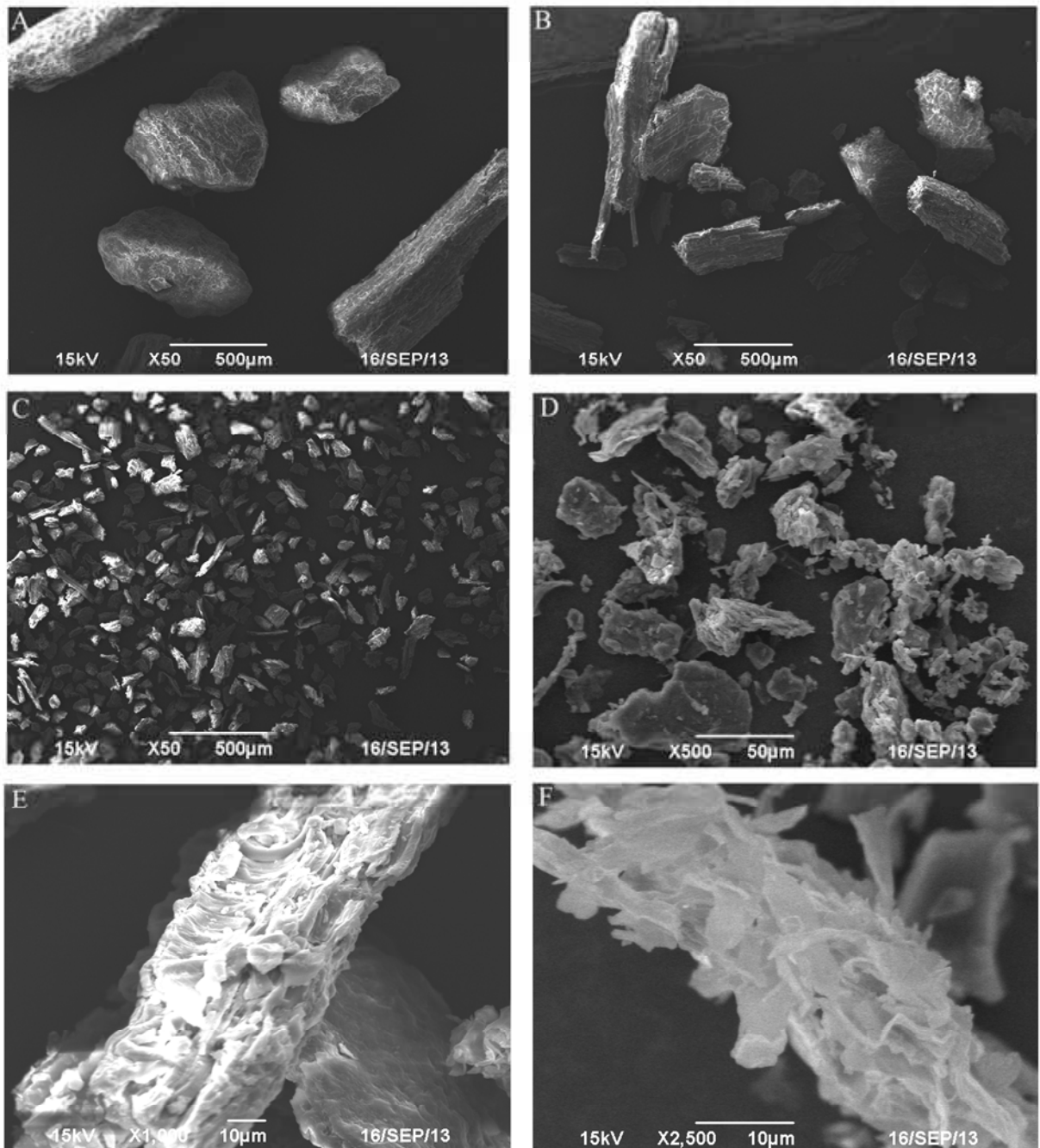


486

487

488 **Fig.2** SEM images of different particle size okra powders. (A) Particle size 380-250489  $\mu\text{m}$ , 50 $\times$ ; (B) Particle size 250-75  $\mu\text{m}$ , 50 $\times$ ; (C) Particle size 75-40  $\mu\text{m}$ , 50 $\times$ ; (D)490 Particle size <40  $\mu\text{m}$ , 500 $\times$ ; (E) Particle size 75-40  $\mu\text{m}$ , 1,000 $\times$ ; (F) Particle size <40491  $\mu\text{m}$ , 2,500 $\times$ .

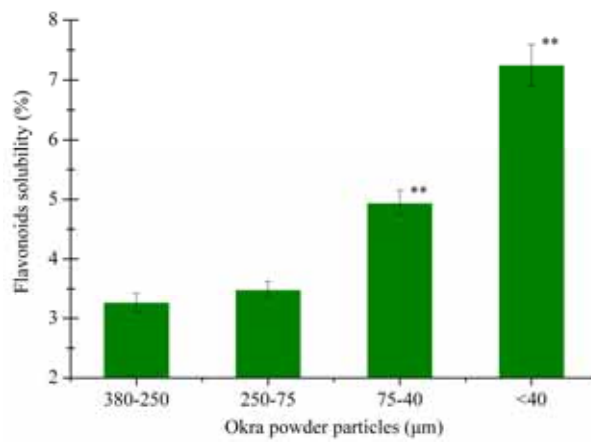
492



493

494

495 **Fig.3** The change of the solubility percentage of flavonoids of different particle size  
496 okra powders.  
497

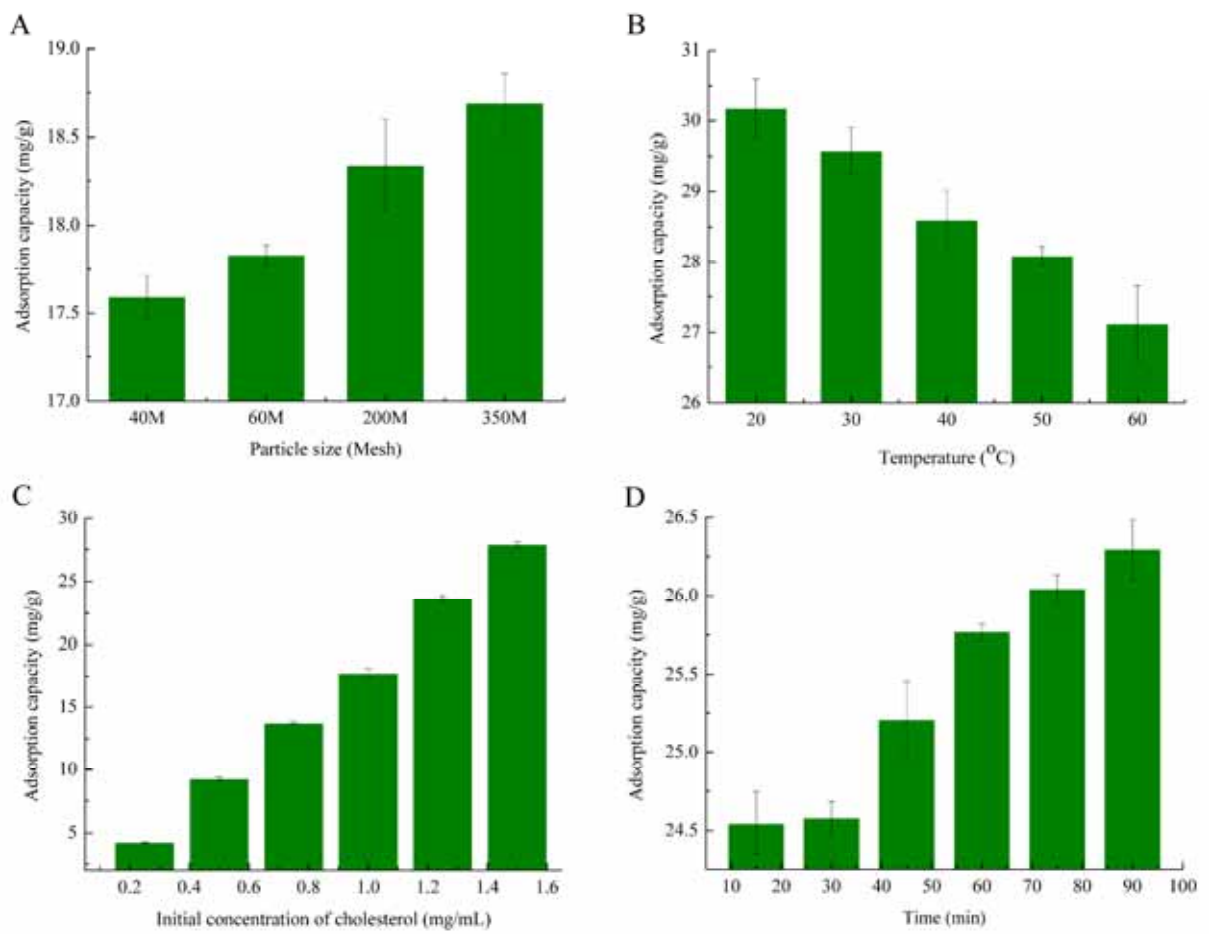


498

499

500 Values are expressed as means  $\pm$  SD (n = 3). Statistical analysis was performed using ANOVA. \*\*  
501 means significantly different from the value of 380-250 $\mu\text{m}$ . (p < 0.01).

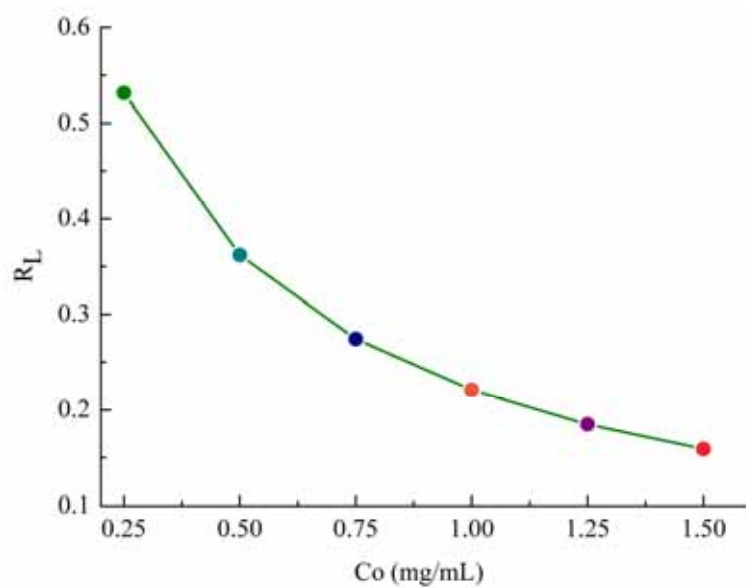
502 **Fig. 4** The effect of particle size(A), temperature(B), initial concentration(C) and  
503 absorption time(D) on cholesterol absorption capacity of okra powder  
504



505

506

507 **Fig. 5** The balance coefficient  $R_L$  for Langmuir isotherm  
508



509